

Article

Characterization and Identification of Varnishes on Copper Alloys by Means of UV Imaging and FTIR

Miriam Truffa Giachet ^{*}, Julie Schröter ^{*} and Laura Brambilla ^{*}

Haute Ecole Arc Conservation Restauration, HES-SO University of Applied Sciences and Arts Western Switzerland, 2000 Neuchâtel, Switzerland

^{*} Correspondence: miriam.truffagiachet@gmail.com (M.T.G.); julie.schroter@he-arc.ch (J.S.); laura.brambilla@he-arc.ch (L.B.); Tel.: +41-32-930-19-19

Abstract: The application of varnishes on the surface of metal objects has been a very common practice since antiquity, both for protective and aesthetic purposes. One specific case concerns the use of tinted varnishes on copper alloys in order to mimic gilding. This practice, especially flourishing in the 19th century for scientific instruments, decorative objects, and liturgical items, results in large museum collections of varnished copper alloys that need to be preserved. One of the main challenges for conservators and restorers deals with the identification of the varnishes through non-invasive and affordable analytical techniques. We hereby present the experimental methodology developed in the framework of the LacCA and VERILOR projects at the Haute École ARC of Neuchâtel for the identification of gold varnishes on brass. After extensive documentary research and analytical campaigns on varnished museum objects, various historic shellac-based varnishes were created and applied by different methods on a range of brass substrates with different finishes. The samples were then characterized by UV imaging and infrared spectroscopy before and after artificial ageing. The comparative study of these two techniques was performed for different thicknesses of the same varnish and for different shellac grades in order to implement an identification methodology based on simple non-invasive examination and analytical tools, which are accessible to conservators.

Keywords: varnishes; shellac; copper alloys; UV-induced fluorescence; FTIR spectroscopy; eddy current; UV imaging; artificial ageing; non-invasive characterization



Citation: Truffa Giachet, M.; Schröter, J.; Brambilla, L. Characterization and Identification of Varnishes on Copper Alloys by Means of UV Imaging and FTIR. *Coatings* **2021**, *11*, 298. <https://doi.org/10.3390/coatings11030298>

Academic Editor: Nervo Marco

Received: 19 February 2021

Accepted: 3 March 2021

Published: 5 March 2021

Publisher's Note: MDPI stays neutral with regard to jurisdictional claims in published maps and institutional affiliations.



Copyright: © 2021 by the authors. Licensee MDPI, Basel, Switzerland. This article is an open access article distributed under the terms and conditions of the Creative Commons Attribution (CC BY) license (<https://creativecommons.org/licenses/by/4.0/>).

1. Introduction

The application of coatings on metal surfaces, especially on copper alloys, is an ancient procedure already in practice since antiquity [1]. Decorative objects, liturgical items, and scientific instruments in particular were often varnished mainly as a protection against corrosion and for esthetic purposes. As copper alloys can naturally exhibit a more or less yellow hue, it is easy to give a golden shine to the surface by applying a tinted transparent coating on the metal substrate. The application of gold varnishes on decorative bronze objects in order to mimic gilding is attested since the 17th century in France [2], although Theophilus mentions the application of a yellow varnish on tin decorative leaves already in the 12th century [3]. The so-called “gilt bronzes”, a misleading appellation referring most of times to brass alloys, are hence very common in museum collections and they need to be preserved. In reason of the optical illusion created by gold varnishes on the surface, one of the main challenges for conservators is the ability to systematically discriminate them from genuine gold layers without the use of complex techniques of characterization. Moreover, the surface is sometimes too strongly worn off to come to a hasty conclusion.

It is in this framework that LacCa and VERILOR projects came about at the Haute École ARC of Neuchâtel. The LacCA project was dedicated to the elaboration of a protocol of identification and characterization of lacquered copper alloys using simple affordable methods, accessible to conservators, as well as sophisticated characterization methods. The current project VERILOR focuses, on the other hand, on gold varnishes found on

decorative bronze objects dating from the 19th century. This project includes the possible presence of restoration materials on the surfaces in order to integrate the identification and characterization protocol outlined in LacCa. Furthermore, historical aspects are explored more in-depth in order to provide a better understanding of the cultural significance of these surface finishes and to be able to preserve them more efficiently.

An extensive 19th century literature review provided information about the materials and methods used to manufacture the objects. Statistics on gold lacquers recipes show that alcohol-based varnishes containing shellac and dyes were the most commonly used to imitate gilding on copper alloys. Shellac is a naturally brownish resin secreted by the female lac bug on trees in the forests of India and comes in various grades depending on the level of purity, bleaching, and dewaxing [4]. The shellac-based varnishes were tinted using a high variety of natural dyes, such as turmeric, sandarac, elemi, saffron, dragon's blood, as well as the first synthetic aniline-based colorants in the second half of the 19th century. These varnishes were then filtered to obtain perfectly transparent coatings.

The investigation of these recipes was firstly approached by the study of pure shellac films of different grades before exploring more complex mixtures including other binding media and colorants. The aim of the article is to study the effectiveness of standard examinations techniques used by conservators (i.e., UV imaging), as well as more complex characterization methods (i.e., FTIR—Fourier-transform infrared spectroscopy) in order to identify pure shellac-based varnishes on copper alloys. The correlation between the two techniques is explored for different grades of shellac varnishes applied in various thicknesses on mock-up samples, including the artificial ageing of the coupons as well. The general overview and methodological aspects of part of this study were presented during the ICOM-CC metals working group conference in 2019 and published in [5].

The examination of objects under UV light is one of the classic, simple, and practical investigation techniques used by conservators and restorers to verify the presence of fluorescent materials non detectable under white light [6–8]. Although databases including the UV fluorescence of materials exist [4,9–11], few studies have been done specifically on gold varnishes applied on copper alloys from the 19th century [12–14]. As for infrared spectroscopy, this technique has proven to be excellent in the identification of complex organic compounds, as well as in the discrimination of different organic materials used as coatings in art [15,16]. Studies of varnishes on metal substrate by FTIR include [13,17,18].

2. Materials and Methods

2.1. Sample Preparation

Various experimental series of samples were created in the framework of the LacCA and VERILOR projects exploring the identification of transparent varnishes on copper alloys. The variables taken into account were the type and the finish of the metal substrate, the nature of the varnish applied, the varnish application method, and the thickness of the varnished layer. The characteristics of the 24 samples selected for comparison are listed in Table 1.

The selected brass coupons are made from CuZn36 and CuZn37 alloys and they were treated to obtain two surface finishes, namely mirror-polish and brush finish (“satin”).

Various varnish recipes were selected based on extensive bibliographic research from a repertory of over 100 recipes [5]; all selected varnishes are shellac-based because of their high occurrence in the 19th century literature; ethanol was used as solvent for the same reason. Different grades of shellac were chosen for comparison (Table 2), namely bleached dewaxed shellac in flakes, orange shellac in flakes (both with wax and dewaxed), and dewaxed seedlac in grains by Kremer Pigmente, as well as three industrial bleached dewaxed shellac products, i.e., “Astra” from Laverdure (in flakes), “Astra” from Boesner (liquid), and “Platina” from Laverdure (in flakes). In addition, a sample of pure shellac wax from Kremer Pigmente was created by melting the wax directly on the coupon on a hot plate.

Table 1. Characteristics of the samples analyzed in this study. Varnish recipes are presented in Table 2. Sample code interpretation: 1st letter = type of substrate finish (S = satin, M = mirror-polished); 2nd (and 3rd) letter = coating technique (md = manual dip-coating; id = industrial dip-coating; b = brush; m = melting); letter between underscore and dash = varnish recipe; after the dash (when present) = to discriminate between samples' duplicates.

Sample Code	Substrate Finish	Varnish Recipe	Coating Technique	Number of Layers	Artificial Ageing (Hours)
Smd_A	Satin		Manual dip-coating	1	-
Mmd_A	Mirror-polish	A	Manual dip-coating	1	-
Mb_A	Mirror-polish		Brush	1	-
Sb_A	Satin		Brush	1	-
Mid_A-2	Mirror-polish		Industrial dip-coating	1	-
Mid_A-11	Mirror-polish		Industrial dip-coating	1	-
Smd_B	Satin	B	Manual dip coating	1	-
RM	Mirror-polish	-	Not varnished	-	-
RS	Satin	-	Not varnished	-	-
Sb_1L-a	Satin	1L	Brush	1	1512
Sb_1L-b					-
Sb_1L-c	Satin	1L	Brush	2	1512
Sb_1L-d					-
Sb_2L-a	Satin	2L	Brush	1	1512
Sb_2L-b					-
Sb_2L-c	Satin	2L	Brush	2	1512
Sb_2L-d					-
Sb_8V-a	Satin	8V	Brush	1	1415
Sb_8V-b					-
Smd_1L-ast	Satin	1L	Manual dip-coating	1	1415
Smd_AS	Satin	AS *	Manual dip-coating	1	1415
Smd_1L-pla	Satin	1L	Manual dip-coating	1	1415
RS-1	Satin	-	Not varnished	-	1415
Sm_SW	Satin	SW **	Melting	1	-

* "Astra" shellac by Boesner, liquid and ready-to-use (not listed in Table 2, see main text). ** Industrial shellac wax, not diluted in ethanol (not listed in Table 2, see main text).

Table 2. Varnish recipes listed in Table 1.

Ingredients	A	B	1L	2L	8V
Bleached dewaxed shellac	125 g	-	225 g	-	-
Orange non-dewaxed shellac	-	225 g	-	-	-
Orange dewaxed shellac	-	-	-	225 g	-
Dewaxed seedlac	-	-	-	-	63 g
Ethanol	2 kg	1 L	1 kg	1 kg	1 L

The varnishes were created by dissolving the shellac in ethanol in a water bath at 50 °C on a heating magnetic stirrer. Different ethanol grades were used depending on the original experimental goals. Coupons varnished with recipes A and B were in fact created to evaluate the spectral response and the thicknesses of the purest shellac varnish possible, and they were therefore fabricated with 99% grade ethanol. The other samples were created to replicate the historical recipes as accurately as possible, and they were therefore produced using less pure ethanol (96%). After preparation, the solutions were vacuum filtered using Büchner flask and funnel and Whatman paper filters (grade 602 h). Recipe B orange shellac was not dewaxed, whereas recipe 2L orange shellac and seedlac were dewaxed using the traditional decanting technique to obtain a completely transparent varnish. The solutions were left several days to decant, and the upper clear liquid was then carefully transferred into clean bottles to be stored in the dark. The Kremer Pigmente, Laverdure, and Boesner bleached shellac, on the contrary, were already industrially dewaxed.

Three coating methods were employed to apply the varnishes on the coupons: manual dip coating, brush application, and industrial dip coating. The first two traditional methods, widely mentioned in the literature [19,20], were chosen to simulate the thinnest varnish layer possible. On the other hand, automated dip coating was performed in order to obtain a homogenous coating layer of known thickness. The details of these application methods can be found in [5]. Two layers of varnish were applied by brush on some sample (Table 1) in order to simulate thicker coatings that could be found on historical objects. Before varnishing, the coupons surface was treated in two ways: the satin coupons destined for recipes A and B and for shellac wax and the mirror-polished coupons were degreased with ethanol with a soft cloth, whereas the other coupons were scraped with powdered pumice stone by means of a toothbrush, rinsed with tap water, then left for few minutes in a bath of sulfuric acid 0.1 M, rinsed again and finally degreased in ethanol and dried. This procedure was performed in order to eliminate possible oxidation products present on the surface, according to procedures found in the literature [21]. As the samples were not heavily tarnished, the coupons were cleaned in one step and not stripped heavily before using several chemical solutions as it is done for freshly cast brass ornaments.

After coating, the samples were left to dry for few days away from contamination and then stocked in transparent boxes to be stored in the dark.

2.2. Artificial Ageing

Some of the samples were placed in a climate chamber in order to evaluate possible changes of the varnishes with the ageing. Natural resins, in fact, have shown changes in some of their physical and chemical characteristics with ageing, as for example in their type of fluorescence under UV light [22,23]. It was therefore chosen to submit some of the samples to accelerated weathering by UV radiation in order to simulate the damaging light exposure conditions to which historic decorative objects and scientific instrument might be exposed indoors.

The samples were placed for 2 months (the total number of hours for each sample is indicated in Table 1) in a Memmert ICH L climate chamber (Memmert GmbH + Co. KG, Büchenbach, Germany) at 50% relative humidity and 25 °C temperature to replicate the average indoor environmental conditions. The two Sylvania Blacklight BL368 UV tubes (Feilo Sylvania, Budapest, Hungary) placed on the upper part of the chamber emit in the UVA spectral range (315–400 nm), with an emission peak at 368 nm. These values are in line with the ISO exposure recommendation for paintings and varnishes [24] and they simulate the portion of the UV daylight not being filtered by common glass windows. The coupons were placed side by side to cover the whole surface of the chamber and they were arranged in order to have the best reproducibility in exposure.

2.3. Characterization Methods

2.3.1. Thickness Measurements

The thickness of the samples was measured with a Phynix Surfex Pro S gauge and FN 1.5 eddy-current probe (PHYNIX GmbH & Co. KG, Neuss, Germany) with a measurement range of 0–1.5 mm and an accuracy, with foil calibration, of $\pm 1.0 \mu\text{m} + 1\%$ of value. All measurements were taken in the same areas of each sample by means of paper masks created according to the size of the coupon. The accuracy of this technique was assessed through a comparative study with spectroscopic ellipsometry and confocal microscopy on the samples varnished with recipes A and B [5].

2.3.2. UV Imaging

Imaging under UV light was performed on all samples with an unfiltered Canon EOS 750D camera (Canon INC, Tokyo, Japan) with an 18–35 mm lens, a Baader UV/IR cut (Baader Planetarium, Munich, Germany) and an X-Nite CC1 filter (LDP LLC, Carlstadt, NJ, USA). The samples, placed on a black non-UV emitting cardboard background, were illuminated by two Dutscher UV lamps (Dominique DUTSCHER SAS, Bernolsheim, France) with emission peak at 365 nm mounted at 45° on a custom-made stand. An UV Innovations target was used as reference in order to later calibrate the pictures in Adobe Photoshop. The pictures were taken in manual mode, ISO 200 and $f/11$ aperture; the target was photographed with 1 s exposure time, whereas the samples with 30 s exposure time. This choice was made in order to be able to see the fluorescence of even the thinnest layers of varnish, otherwise not visible with shorter exposure times. White balance correction was performed on the pictures in Adobe Photoshop Camera Raw following the Adobe Photoshop Setup and Capture Workflows recommended by the target manufactures (<https://www.uvinnovations.com/getting-started> (accessed on March 2018)). No exposure correction was applied to the samples. $L^* a^* b^*$ values of three spots ($11 \text{ px} \times 11 \text{ px}$) were then recorded for each coupon in Adobe Photoshop using the color sampling tool in order to compare the color of the fluorescence of each varnish.

2.3.3. Fourier-Transform Infrared Spectroscopy

All samples were analyzed with a ThermoFischer Scientific Nicolet iS 5 FTIR spectrometer (ThermoFischer Scientific, Waltham, MA, USA) in reflectance mode. Spectra were collected using 128 scans at 4 or 8 cm^{-1} resolution, measuring between 4000 and 650 cm^{-1} . A custom-made external module was used to be able to compare the coupons spectra with those obtained from museum objects analyzed with the same configuration (Figure 1). Coupons varnished with recipe 8V were also analyzed with a benchtop ThermoFischer Scientific Nicolet iN 10 MX FTIR microscope (ThermoFischer Scientific, Waltham, MA, USA) with the same collection parameters in order to have better spectral response.

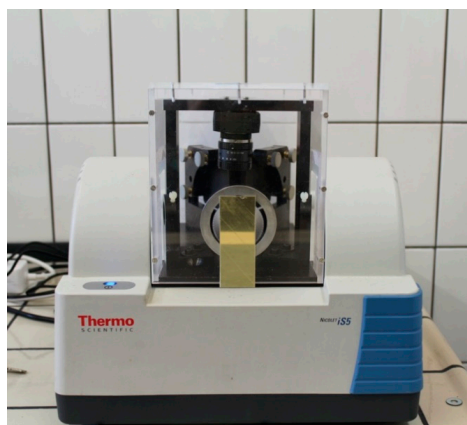


Figure 1. The FTIR instrument with custom-made external module used to analyze the samples.

Baseline correction and atmospheric suppression were applied to the raw FTIR spectra.

3. Results

3.1. Thickness Measurement

Table 3 shows the average thickness of the samples measured with an eddy-current probe.

Table 3. Average thickness of the samples obtained by eddy-current probe. Standard deviation at 1σ .

Code	Average Thickness (μm)
Smd_A	0.7 ± 0.3
Mmd_A	1.0 ± 0.2
Mb_A	0.7 ± 0.2
Sb_A	0.9 ± 0.2
Mid_A-2	2.1 ± 0.3
Mid_A-11	11.2 ± 0.6
Smd_B	1.3 ± 0.2
Sb_1L-a	3.3 ± 0.2
Sb_1L-b	2.8 ± 0.3
Sb_1L-c	5.0 ± 0.2
Sb_1L-d	3.8 ± 0.2
Sb_2L-a	1.3 ± 0.1
Sb_2L-b	1.4 ± 0.2
Sb_2L-c	2.1 ± 0.3
Sb_2L-d	1.8 ± 0.4
Sb_8V-a	1.4 ± 0.5
Sb_8V-b	1.4 ± 0.3
Smd_1L-ast	1.4 ± 0.1
Smd_AS	11.8 ± 0.4
Smd_1L-pla	1.3 ± 0.2
Sm_W	50.3 ± 13.9

Free-hand measurements with eddy-current probe resulted to be precise after adequate calibration with thin foil [5].

3.2. UV Imaging and Colorimetry

Figure 2 shows the fluorescence under UV light and the $L^*a^*b^*$ colorimetric coordinates of the different types of shellac varnishes, the shellac wax, and the not-varnished sample. Samples Sb_A, Sb_1L-b, Sb_8V-a, and Sb_2L-b were varnished by brush, whereas varnish on samples Smd_1L-ast, Smd_1L-pla, and Smd_AS was applied by manual dip-coating.

Figure 3 shows how samples varnished with recipe A, 1L, and 2L, sorted by mode of varnish application and thickness of the layer applied, appear under UV light in comparison with non-varnished reference coupons; the $L^* a^* b^*$ colorimetric coordinates of the fluorescence of the varnishes on different supports and with different thicknesses obtained in Adobe Photoshop are listed as well.

Figure 4 shows how samples with different varnishes appear under UV light before and after artificial ageing, taking into account the $L^* a^* b^*$ colorimetric coordinates and the thickness of the varnishes. Due to the improvement and the changes of the UV imaging setup during the experiments, it was not possible to compare the same coupon before and after ageing for varnishes 1L and 2L. A non-aged duplicate of each type was therefore used as the “before ageing” sample.

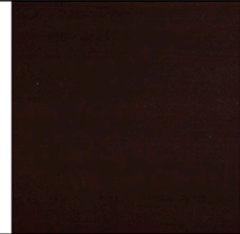
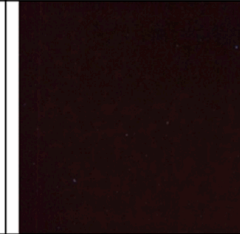
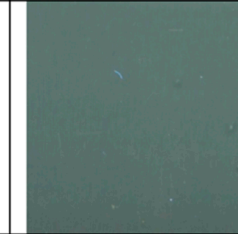
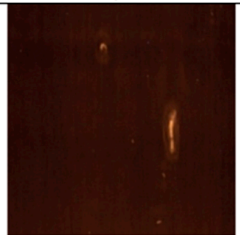
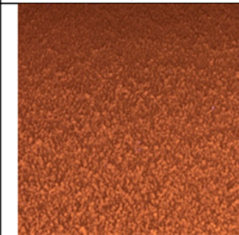
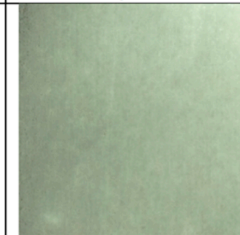
Bleached dewaxed shellac	Bleached dewaxed shellac	Bleached dewaxed shellac	Bleached dewaxed shellac	Bleached dewaxed shellac
Recipe A	Recipe 1L	Recipe 1L	Recipe 1L	Ready-to-use
				
Sb_A	Sb_1L-b	Smd_1L-ast	Smd_1L-pla	Smd_AS
$0.9 \pm 0.2 \mu\text{m}$	$2.8 \pm 0.3 \mu\text{m}$	1.4 ± 0.1	1.3 ± 0.2	11.8 ± 0.4
$L^* = 11 \pm 1$	$L^* = 11 \pm 1$	$L^* = 9 \pm 1$	$L^* = 6 \pm 1$	$L^* = 46 \pm 1$
$a^* = 4 \pm 1$	$a^* = 6 \pm 1$	$a^* = 7 \pm 1$	$a^* = 4 \pm 1$	$a^* = -7 \pm 0$
$b^* = 4 \pm 1$	$b^* = 5 \pm 1$	$b^* = 3 \pm 1$	$b^* = 4 \pm 1$	$b^* = 0 \pm 1$
Dewaxed seedlac	Orange dewaxed shellac	Orange non-dewaxed shellac	Shellac wax	Not-varnished sample
Recipe 8V	Recipe 2L	Recipe B	Ready-to-use	-
				
Sb_8V-a	Sb_2L-b	Smd_B	Sm_W	RS-1
1.4 ± 0.1	$1.4 \pm 0.2 \mu\text{m}$	1.3 ± 0.2	50.3 ± 13.9	-
$L^* = 10 \pm 2$	$L^* = 17 \pm 1$	$L^* = 42 \pm 9$	$L^* = 72 \pm 6$	$L^* = 2 \pm 0$
$a^* = 12 \pm 0$	$a^* = 15 \pm 1$	$a^* = 25 \pm 3$	$a^* = -9 \pm 1$	$a^* = 3 \pm 1$
$b^* = 10 \pm 2$	$b^* = 17 \pm 1$	$b^* = 30 \pm 5$	$b^* = 12 \pm 2$	$b^* = 0 \pm 0$

Figure 2. Results of the UV imaging and the colorimetric analysis performed on samples with different grades of shellac.

3.3. Fourier-Transform Infrared Spectroscopy

Figure 5 shows the FTIR spectra of the representative samples of each varnish recipe: samples Mb_A (recipe A), Sb_1L-d (recipe 1L), Smd_1L-ast (“Astra”), Smd_1L-pla (“Platina”), and Smd_AS (“Astra”, ready-to-use) for bleached dewaxed shellac; samples Smd_B (recipe B) and Sb_2L-d (recipe 2L) for orange shellac; sample Sb_8V-b (recipe 8V) for seedlac; Sm_W for shellac wax.

Figure 6 shows the FTIR spectra of samples before and after ageing. Spectra Sb_8V-a and Sb_8V-b were acquired with the benchtop instrument in order to obtain better spectral response (cf. 2.3.3).

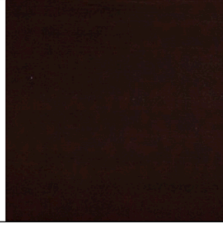
Bleached dewaxed shellac		Bleached dewaxed shellac	
Recipe A, manual dip-coating		Recipe A, industrial dip-coating	
			
Mmd_A	Smd_A	Mid_A-2	Mid_A-11
1.0 ± 0.2 μm	0.7 ± 0.3 μm	2.1 ± 0.3 μm	11.2 ± 0.6 μm
$L^* = 6 \pm 1$	$L^* = 7 \pm 1$	$L^* = 13 \pm 0$	$L^* = 33 \pm 1$
$a^* = 2 \pm 1$	$a^* = 5 \pm 1$	$a^* = 4 \pm 0$	$a^* = 7 \pm 1$
$b^* = -6 \pm 0$	$b^* = -2 \pm 1$	$b^* = 5 \pm 1$	$b^* = 12 \pm 1$
Bleached dewaxed shellac		Bleached dewaxed shellac	
Recipe A, brush application		Recipe 1L, brush application	
			
Mb_A	Sb_A	Sb_1L-b	Sb_1L-d
0.7 ± 0.2 μm	0.9 ± 0.2 μm	2.8 ± 0.3 μm	3.8 ± 0.2 μm
$L^* = 10 \pm 1$	$L^* = 11 \pm 1$	$L^* = 11 \pm 1$	$L^* = 19 \pm 1$
$a^* = 2 \pm 1$	$a^* = 4 \pm 1$	$a^* = 6 \pm 1$	$a^* = 5 \pm 1$
$b^* = 5 \pm 0$	$b^* = 4 \pm 1$	$b^* = 5 \pm 1$	$b^* = 7 \pm 1$
Orange dewaxed shellac		Not-varnished references	
Recipe 2L, brush application			
			
Sb_2L-b	Sb_2L-d	RM	RS
1.4 ± 0.2 μm	1.8 ± 0.4 μm	-	-
$L^* = 17 \pm 1$	$L^* = 25 \pm 1$	$L^* = 2 \pm 1$	$L^* = 2 \pm 0$
$a^* = 15 \pm 1$	$a^* = 18 \pm 1$	$a^* = 4 \pm 0$	$a^* = 4 \pm 0$
$b^* = 17 \pm 1$	$b^* = 23 \pm 1$	$b^* = 1 \pm 1$	$b^* = 0 \pm 1$

Figure 3. Results of the UV imaging and the colorimetric analysis performed on varnishes with different thicknesses and on different supports.

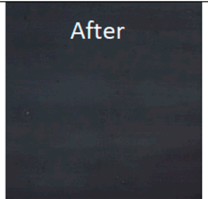
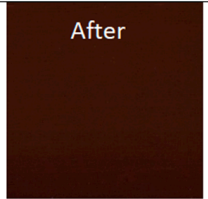
Bleached dewaxed shellac		Bleached dewaxed shellac		Orange dewaxed shellac	
Varnish 1L		Varnish 1L		Varnish 2L	
					
Sb_1L-b	Sb_1L-a	Sb_1L-d	Sb_1L-c	Sb_2L-b	Sb_2L-a
2.8 ± 0.3 μm	3.3 ± 0.2 μm	3.8 ± 0.2 μm	5.0 ± 0.2 μm	1.4 ± 0.2 μm	1.3 ± 0.1 μm
$L^* = 11 \pm 1$	$L^* = 12 \pm 0$	$L^* = 19 \pm 1$	$L^* = 24 \pm 1$	$L^* = 17 \pm 1$	$L^* = 14 \pm 1$
$a^* = 6 \pm 1$	$a^* = 3 \pm 1$	$a^* = 5 \pm 1$	$a^* = 0 \pm 0$	$a^* = 15 \pm 1$	$a^* = 13 \pm 1$
$b^* = 5 \pm 1$	$b^* = -2 \pm 0$	$b^* = 7 \pm 1$	$b^* = -4 \pm 0$	$b^* = 17 \pm 1$	$b^* = 13 \pm 1$
Orange dewaxed shellac		Dewaxed seedlac		Bleached dewaxed shellac	
Varnish 2L		Varnish 8V		Varnish 1L	
					
Sb_2L-d	Sb_2L-c	Sb_8V-a		Smd_1L-pla	
1.3 ± 0.1 μm	2.1 ± 0.3 μm	1.4 ± 0.5 μm		1.3 ± 0.2 μm	
$L^* = 25 \pm 1$	$L^* = 25 \pm 0$	$L^* = 10 \pm 2$	$L^* = 9 \pm 1$	$L^* = 6 \pm 1$	$L^* = 7 \pm 1$
$a^* = 18 \pm 1$	$a^* = 18 \pm 0$	$a^* = 12 \pm 0$	$a^* = 9 \pm 1$	$a^* = 4 \pm 1$	$a^* = 4 \pm 1$
$b^* = 23 \pm 1$	$b^* = 23 \pm 0$	$b^* = 10 \pm 2$	$b^* = 8 \pm 2$	$b^* = 4 \pm 1$	$b^* = 4 \pm 1$
Bleached dewaxed shellac		Bleached dewaxed shellac		Not-varnished reference	
Varnish ready-to-use		Varnish 1L			
					
Smd_AS		Smd_1L-ast		RS-1	
11.8 ± 0.4 μm		1.4 ± 0.1 μm		-	
$L^* = 46 \pm 1$	$L^* = 50 \pm 1$	$L^* = 9 \pm 1$	$L^* = 9 \pm 1$	$L^* = 2 \pm 0$	$L^* = 2 \pm 1$
$a^* = -7 \pm 0$	$a^* = -7 \pm 1$	$a^* = 7 \pm 1$	$a^* = 6 \pm 1$	$a^* = 3 \pm 1$	$a^* = 4 \pm 1$
$b^* = 0 \pm 1$	$b^* = 0 \pm 1$	$b^* = 3 \pm 1$	$b^* = 2 \pm 1$	$b^* = 0 \pm 0$	$b^* = 0 \pm 0$

Figure 4. Results of the UV imaging and the colorimetric analysis performed on samples before and after artificial ageing.

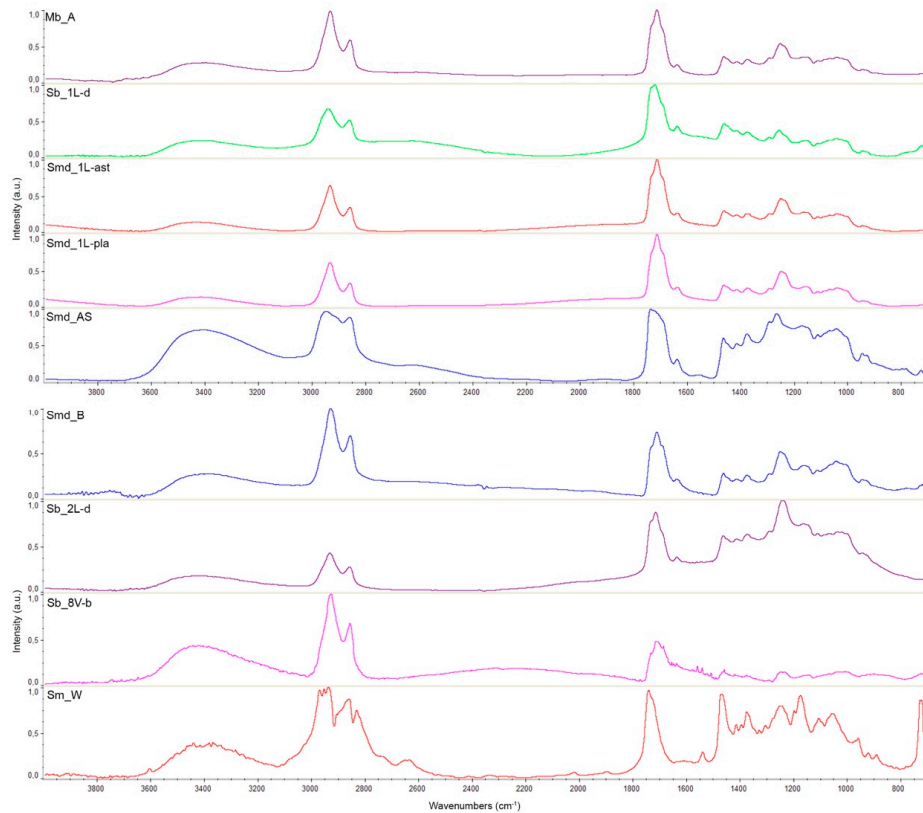


Figure 5. FTIR spectra of the representative samples for each varnish recipe and shellac wax. Spectrum Sb_8V-b was acquired with the benchtop instrument (cf. 2.3.3).

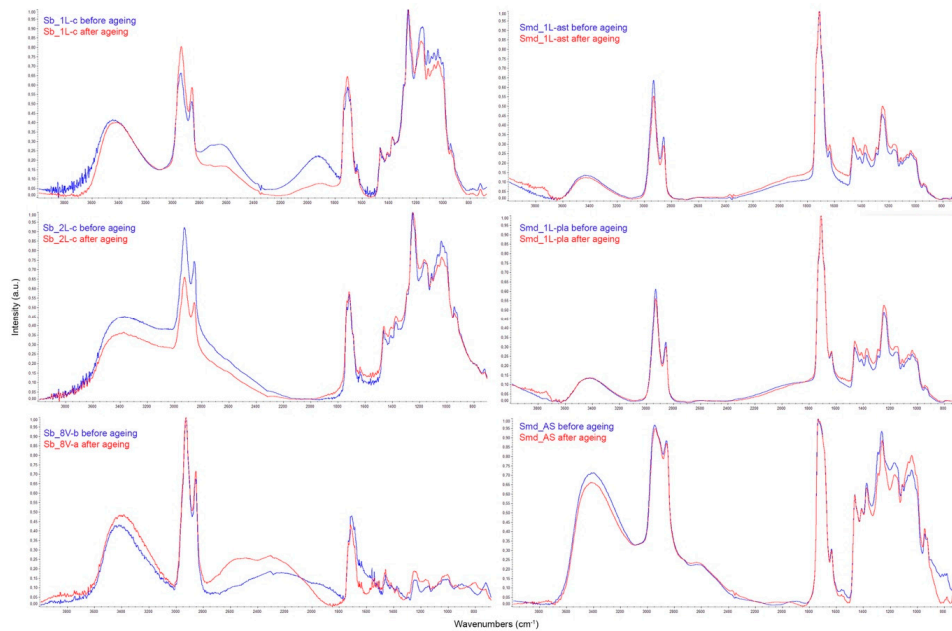


Figure 6. FTIR spectra of the samples before (blue spectra) and after (red spectra) ageing. On the left, from top to bottom: Sb_1L-c, Sb_2L-c, Sb_8V-b (and Sb_8V-a); on the right, from top to bottom: Smd_1L-ast, Smd_1L-pla, Smd_AS.

4. Discussion

4.1. Comparison between Different Grades of Shellac

As shown in Figures 2 and 7, different grades of shellac can be differentiated by their fluorescence under UV light.

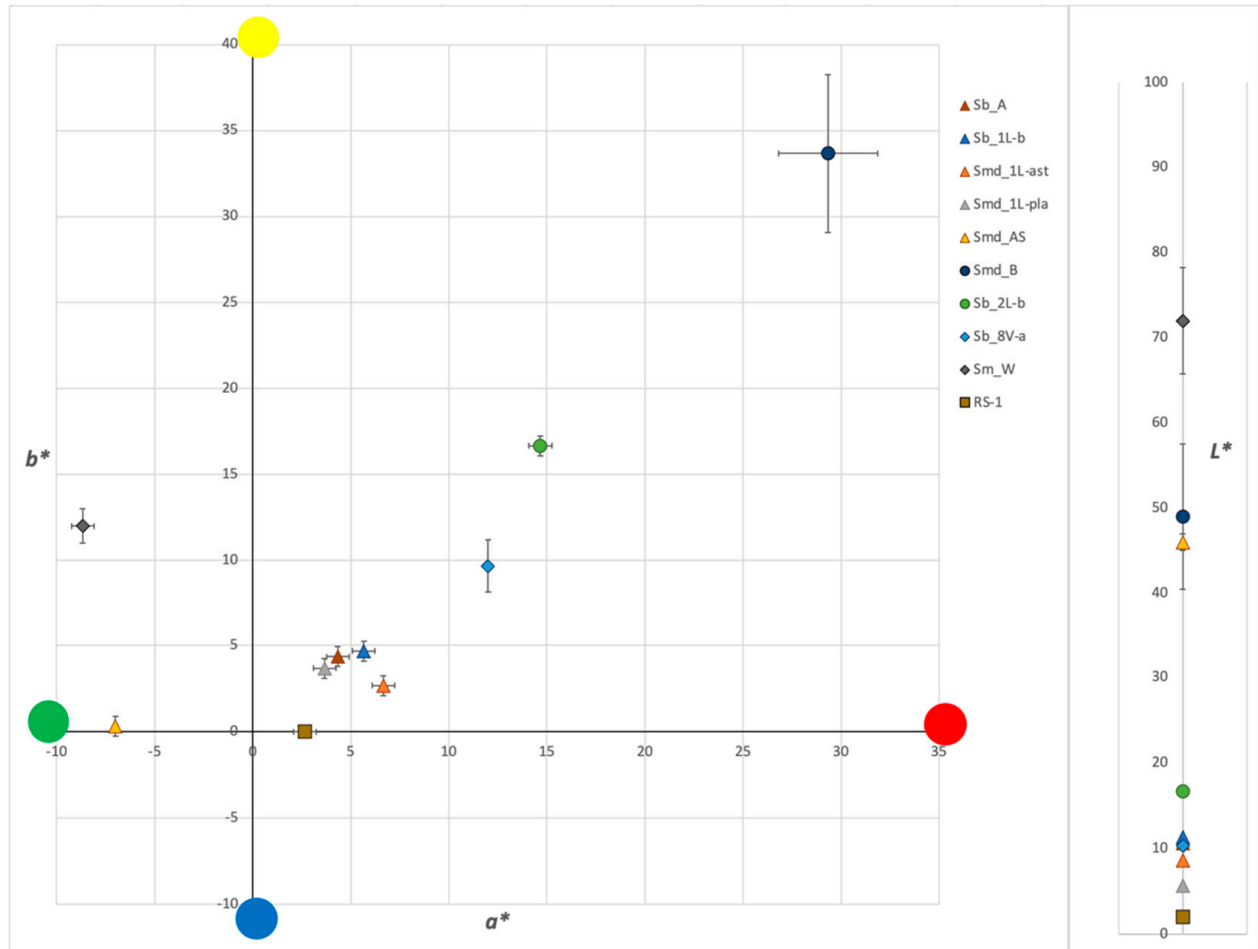


Figure 7. L^* a^* b^* colorimetric coordinates of the varnishes' fluorescence under UV light (cf. Figure 2). ▲: bleached dewaxed shellac; ●: orange shellac with or without wax; ◆: seedlac and shellac wax; ■: non-varnished references.

It is possible to observe that orange shellac and seedlac exhibit a quite visible orange fluorescence, which is stronger when wax is present in the varnish (sample Smd_B): shellac wax is in fact very fluorescent under UV light, as corroborated by the aspect of the pure shellac wax sample Sm_W. On the other hand, bleached dewaxed shellac shows a weak fluorescence tending towards neutral tinges, with the exception of the ready-to-use "Astra" shellac by Boesner (sample Smd_AS), exhibiting a much greener hue. This fluorescence color is usually linked to other natural vegetal resins, such as mastic, dammar, or rosin [4,10,25,26]. The latter is in fact present in traces in this industrial product, as indicated in its ingredients list. This might explain why the FTIR spectrum of the Smd_AS shellac sample is the only one presenting slight variations in comparison to all other pure shellac samples (Figure 8).

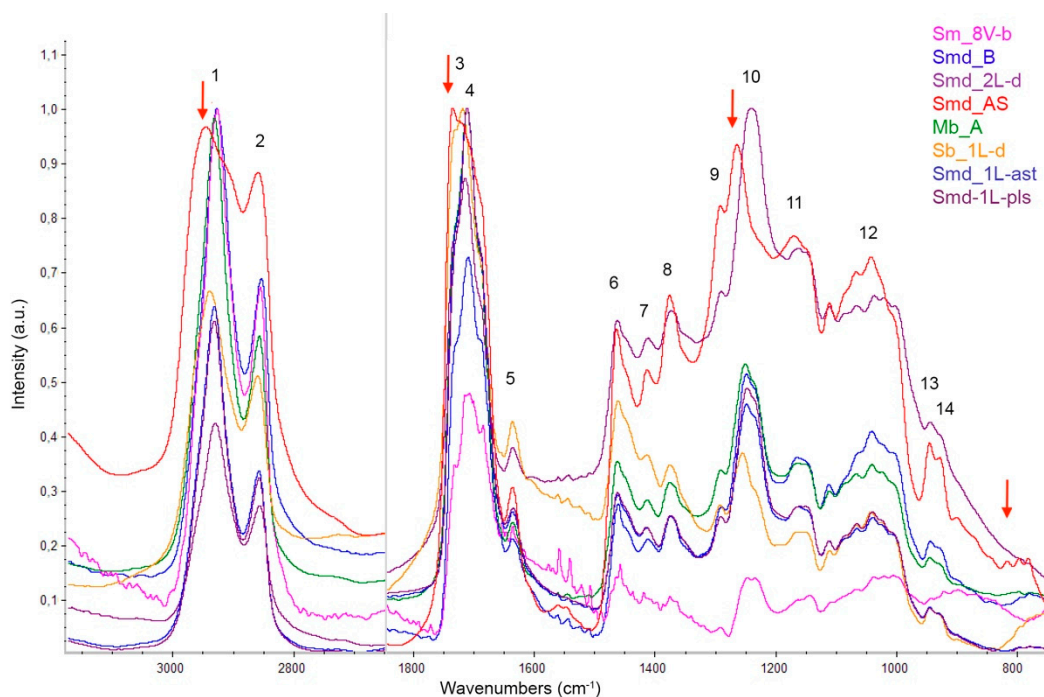


Figure 8. Difference between sample Smd_AS and the other shellac samples analyzed (red arrows). The number of top of the peaks (1–14) refers to peak assignments reported in Table 4.

Table 4. Characteristic peaks of shellac. Peak assignment after [27,28].

Number in Figure 8	Molecular Motion	Wavelength (cm ⁻¹)	Number in Figure 8	Molecular Motion	Wavelength (cm ⁻¹)
1	C–H stretch	2934–2920	8	C–H bend	1377
2	C–H stretch	2857	9	C–O stretch	1291
3	C=O stretch	1730–1738	10	C–O stretch	1240
4	C=O stretch	1715–1722	11	C–O stretch	1163
5	C=C stretch	1636	12	C–O stretch	1040
6	C–H bend	1466	13	C–H stretch	945
7	C–H bend	1412	14	C–H stretch	930

All shellac spectra show the characteristic peaks of this resin (Figure 8 and Table 4).

It is interesting to notice that it is not possible to differentiate between orange and bleached dewaxed shellac varnishes by FTIR (Figure 8), which is instead possible by UV imaging (Figures 2 and 7). These two techniques result hence to be complementary for the characterization of varnishes on copper alloys. However, different types of bleached dewaxed shellac appear similar under UV light in reason of the weak fluorescence of this material, especially in very thin layers (cf. 4.3). It is interesting to observe that, even though differences in hue are very hard to detect with naked eye, variations can be identified in the $L^* a^* b^*$ colorimetric space. Nonetheless, caution must be applied in the interpretation of the results in case of weak fluorescence because even minor changes in the environmental condition during observation might affect the hue and lightness of the resulting color. These changes are on the contrary less noticeable when the fluorescence is strong and very tinted.

As by UV imaging, it is possible to detect by FTIR the presence of wax in the varnish, appearing as a characteristic double peak at 730 and 720 cm⁻¹ [27] (p. 107), [28] (pp. 100–102); these peaks are indeed visible in the non-dewaxed orange varnish B (sample Smd_B) and in shellac wax (sample Sm_W), as well as, partially, in the manually dewaxed shellac varnish 8V (samples Sb_8V-a and Sb_8V-b), which clearly still contains traces of

wax (Figure 9). Wax was instead more efficiently manually removed in varnishes 1L and 2L (samples Sb_1L-d and Sb_2L-d).

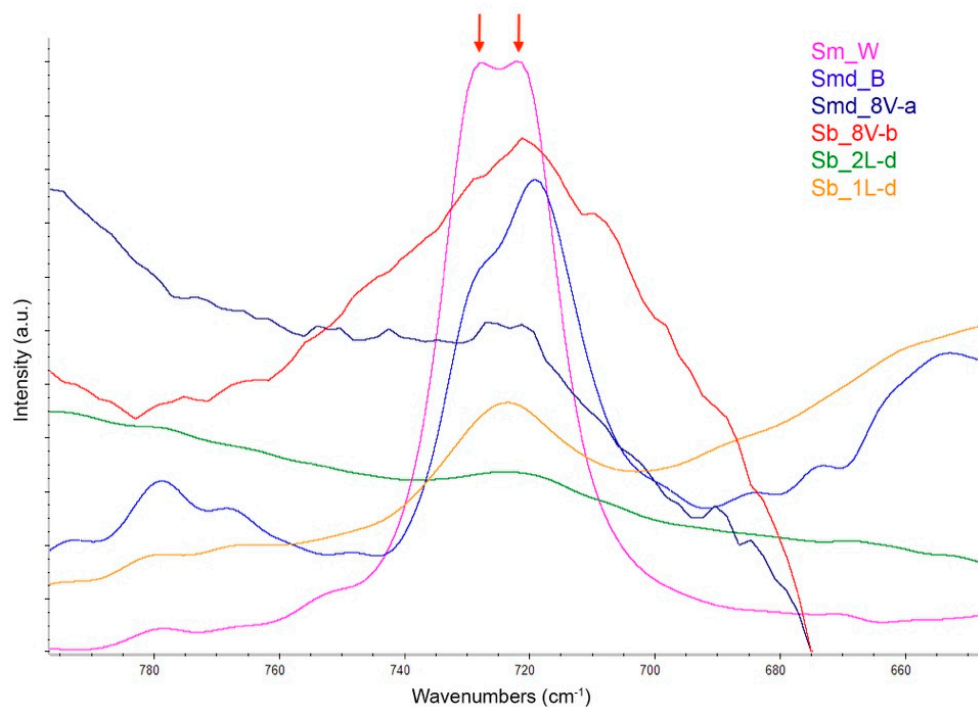


Figure 9. Characteristic peaks of shellac wax.

4.2. Comparison between Various Thicknesses of the Same Varnish

Figures 3 and 10 show that the thickness of the varnish layer affects the intensity of its fluorescence under UV light. Although the fluorescence of bleached dewaxed shellac is not always detectable with naked eye, it is possible to observe that thicker layers of varnish have a higher lightness value (L^*) and are more visible under UV light. Sample Mid_A-11, coated by industrial dip-coating with a varnish layer 11 μm thick, shows in fact the clearest fluorescence among all samples varnished with recipe A. Moreover, the fluorescence color is distinctly visible with naked eye and it is distinguishable from the more orange fluorescence of the raw shellac. On the other hand, it is difficult to discriminate between different types of support and different varnish application modes, especially for very thin layers of varnish. Looking at thicker layers, however, it seems that these two variables do not affect the intensity of the fluorescence, as shown by the similar $L^* a^* b^*$ coordinates of samples Mid_A-2 (mirror-polished substrate, industrial dip-coating) and Sb_1L-b (satin substrate, brush application), both having a varnish thickness of 2 to 3 μm . Nevertheless, it must be kept in mind that external factors might affect in a stronger way weaker fluorescence during observation, as already mentioned in Section 4.1.

Considering the orange dewaxed shellac, the sample coated with two layers of varnish 2L (Sb_2L-d) shows a stronger fluorescence than the sample having one layer (Sb_2L-b).

Concerning the infrared spectroscopy, the thickness of the analyzed layer seems to have an impact on the spectrum quality. Thicker samples lead in fact to the saturation of the C–H and C=O stretching peaks, and a higher thickness might be the cause of an anomalous series of waves deforming the baseline around 3100 cm^{-1} and between 2800 and 1800 cm^{-1} (Figure 11) [29]. More research needs however to be done to confirm this theory.

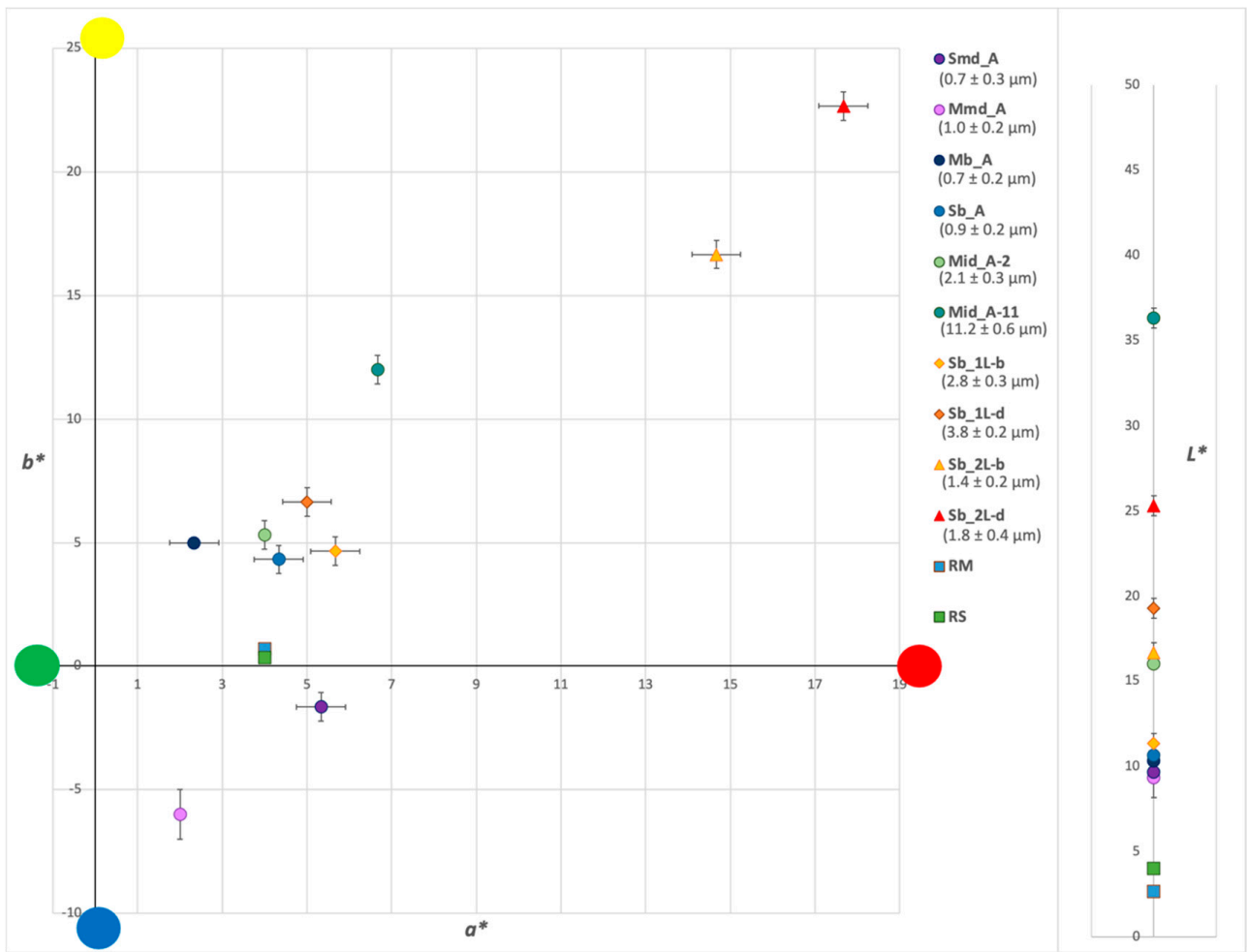


Figure 10. L^* a^* b^* colorimetric coordinates of the fluorescence under UV light of coatings with different thickness (cf. Figure 3). ●: varnish A; ◆: varnish 1L; ▲: varnish 2L; ■: non-varnished references.

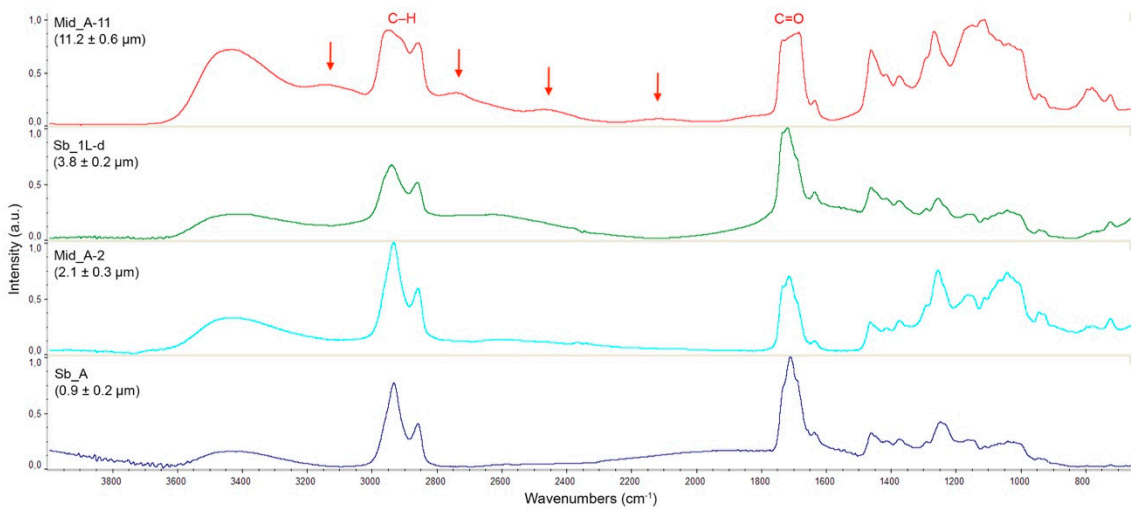


Figure 11. Impact of the thickness on the FTIR spectrum quality. The arrows point to the “waves” indicated in the text.

4.3. Comparison of the Characteristics before and after Artificial Ageing

Plotting the L^* a^* b^* coordinates of the UV fluorescence of the samples before and after ageing (Figure 12, cf. Figure 4) it is possible to see that no change is noticeable for the industrially dewaxed bleached shellac samples with weak fluorescence (Smd_1L-ast and Smd_1L-pla), whereas a slight increase in lightness is found for the thicker and more fluorescent sample Smd-AS. This might be due to the fact that slight changes in hue and lightness are more difficult to detect in case of low fluorescence. On the other hand, samples coated with the manually dewaxed varnishes 1L, 2L, and 8V show a shift towards bluish-greenish hues with ageing, with the exception of the orange shellac applied in two layers (sample Sb_2L-c/-d). The difference is higher for less fluorescent bleached shellac varnish 1L, with ΔE values of 12.8 (Sb_1L-c/-d) and 7.1 (Sb_1L-a/-b), and lower for the more fluorescent unbleached shellac varnishes 2L and 8V, with ΔE values of 4.7 (Sb_2L-a/-b) and 3.6 (Sb_8V-a). It needs to be noted that, as explained in Section 3.2, it was not possible to compare the same sample before and after ageing for varnishes 1L and 2L, which might partially affect the difference in hue of these samples. More research needs to be done on a larger set of samples in order to confirm these preliminary results.

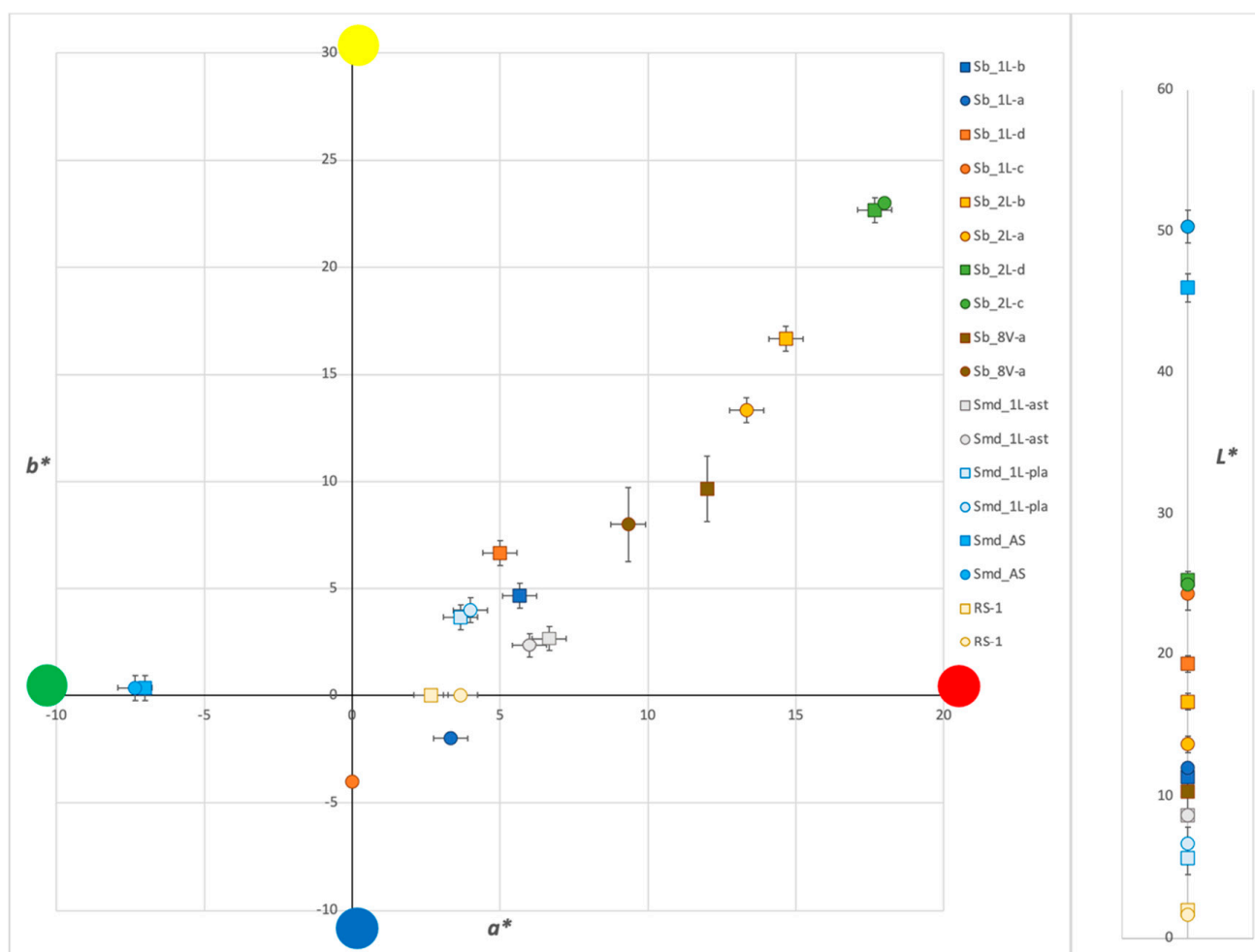


Figure 12. L^* a^* b^* colorimetric coordinates of the varnishes' fluorescence under UV light before (■) and after (●) ageing (cf. Figure 4).

Results of the FTIR analysis, on the other hand, show no difference between the spectra of the samples before and after ageing (Figure 6).

5. Conclusions

The UV imaging and FTIR analysis of mock-up varnished brass coupons allowed the assessment of the effectiveness of these techniques in the identification of different grades of shellac. The observation under UV light of the samples resulted to be an efficient method to discriminate between bleached dewaxed shellac and raw dewaxed shellac; however, the limit of detection of the UV fluorescence of the varnish relates to the thickness of the coating, especially for the more refined resin. For thicknesses $\leq 1 \mu\text{m}$ it is in fact very difficult to detect the presence of bleached dewaxed shellac with naked eye under UV light, although a slight change in the $L^* a^* b^*$ coordinates does occur. This shows the need to use a particularly strong radiation source when it comes to observing objects in situ in order to be able to detect even the thinnest layers. FTIR spectroscopy, on the other hand, proved to be effective in the detection of very thin layers of shellac-based varnishes. Besides, a greater thickness of the coating seems to affect the IR spectrum quality, leading to saturation and deformation of the IR bands. This effect was observed in the present study for varnishes thicker than $10 \mu\text{m}$, but further investigation is necessary to verify the behavior between 2 and $10 \mu\text{m}$. Contrary of the UV imaging, it is not possible to discriminate between different grades of shellac by FTIR spectroscopy. These two techniques proved therefore to be complementary in the detection and identification of shellac varnishes on copper alloys.

From a qualitative point of view, bleached dewaxed shellac fluorescence tends towards neutral colors, whereas orange shellac and seedlac fluorescence exhibits a more orange hue. The presence of additives in the varnish can heavily affect the color of the sample under UV light, as showed by the ready-to-use “Astra” shellac containing traces of rosin and exhibiting a greener fluorescence. Moreover, the presence of shellac wax, easily detectable by FTIR spectroscopy, increases by far the fluorescence of the varnish. It needs to be noted that, when analyzing real artefacts, we focused on the examination of portions of the objects presenting a varnish in a good condition; therefore, no investigation was carried out on the mock-up samples on the possible influence of metal corrosion on the varnish fluorescence under UV light, as well as on the interaction between the varnish and the metal. These factors could further affect the intensity and the color of the varnish fluorescence.

No changes were observed in the FTIR spectra of samples before and after artificial ageing, nor in the UV fluorescence of the majority of the coupons. Some of the varnishes showed a shift towards bluish-greenish hues with ageing but it is not clear how other factors might have affected this result. More research needs to be done on a larger set of samples in order to confirm this result.

Author Contributions: Conceptualization, methodology and validation: M.T.G., L.B. and J.S.; formal analysis and investigation: M.T.G. and L.B.; writing—original draft preparation: M.T.G.; writing—review and editing: M.T.G., L.B. and J.S.; visualization: M.T.G.; supervision: L.B. and J.S.; project administration and funding acquisition: J.S. All authors have read and agreed to the published version of the manuscript.

Funding: This research was funded by the Haute Ecole Spécialisée de Suisse Occidentale, Grant No. 100779/DAV-RAD19-06, and co-funded by Haute Ecole Arc conservation-restauration.

Institutional Review Board Statement: Not applicable.

Informed Consent Statement: Not applicable.

Data Availability Statement: The data presented in this study are available within the article and in [5].

Acknowledgments: The authors would like to thank Laure Jeandupeux, (Haute Ecole Arc, Neuchâtel, Switzerland, medical devices), David Grange (HES professor, Haute Ecole Arc, Neuchâtel, Switzerland), and Stephan Ramseyer (Haute Ecole Arc, Neuchâtel, Switzerland, surface engineering). We would also like to thank the Lathema laboratory of University of Neuchâtel for the use of the FTIR with external module.

Conflicts of Interest: The authors declare no conflict of interest. The funders had no role in the design of the study; in the collection, analyses, or interpretation of data; in the writing of the manuscript, or in the decision to publish the results.

References

1. Halleux, R. *Les Alchimistes grecs. Tome I: Papyrus de Leyde—Papyrus de Stockholm—Recettes*, 3rd ed.; Les belles lettres: Paris, France, 2019.
2. Verlet, P. *Les bronzes dorés français du XVIIIe siècle*; Editions A & J Picard: Paris, France, 1987.
3. Mounier, A.; Daniel, F.; Bechtel, F. L'illusion de l'or. *ArcheoSciences* **2009**, *33*, 397–403. [CrossRef]
4. Perego, F. *Dictionnaire des matériaux du peintre*; Éditions Belin: Paris, France, 2005.
5. Schröter, J.; Michel, A.; Mirabaud, S.; Brambilla, L.; Paris, C.; Bellot-Gurlet, L. Transparent varnishes on copper alloys dating from the 19th century: Characterization and identification strategies. In Proceedings of the interim meeting of the ICOM-CC metals working group, Neuchâtel, Switzerland, 2–6 September 2019.
6. Buzzegoli, E.; Keller, D. Ultraviolet fluorescence imaging. In *Scientific Examination for the Investigation of Paintings: A Handbook for Conservator-Restorers*; Pinna, D., Galeotti, M., Mazzeo, R., Eds.; Centro Di: Florence, Italy, 2009; pp. 204–206.
7. Thackray, A. A methodology for the conservation of furniture mounts. *V A Conserv. J.* **2014**, *62*.
8. Cosentino, A. Practical notes on ultraviolet technical photography for art examination. *Conserv. Património* **2015**, *21*, 53–62. [CrossRef]
9. Measday, D. A summary of ultra-violet fluorescent materials relevant to conservation. *AICCM Natl. Newsl.* **2017**, *137*. Available online: <https://bit.ly/3pjAq8U> (accessed on 10 February 2021).
10. Umney, N.; Rivers, S. *Conservation of Furniture*; Routledge: New York, NY, USA, 2013.
11. The Conservation and Art Materials Encyclopedia Online (CAMEO). Available online: http://cameo.mfa.org/wiki/Category:Materials_database (accessed on 10 February 2021).
12. Thomson, C. Last but not least, examination and interpretation of coatings on brass hardware. In Proceedings of the AIC Annual Meeting, Albuquerque, NM, USA, 3–8 June 1991; pp. 1–15.
13. Long, D. The treatment of false gilding: A case study. In *Gilded Metals: History, Technology and Conservation*; Drayman-Weisser, T., Ed.; Archetype Publications Ltd.: London, UK, 2000; pp. 319–327.
14. Jeanneret, R. Approche Pluridisciplinaire Pour le Traitement de Conservation-Restauration d'un Quart de Cercle Mural du 18ème Siècle du Musée des Confluences de Lyon. Master's Thesis, HES-SO, Neuchâtel, Switzerland, 2010.
15. Galeotti, M.; Joseph, E.; Mazzeo, R.; Prati, S. Transform infrared spectroscopy. In *Scientific Examination for the Investigation of Paintings: A Handbook for Conservator-Restorers*; Pinna, D., Galeotti, M., Mazzeo, R., Eds.; Centro Di: Florence, Italy, 2009; pp. 151–156.
16. Echard, J.-P. Le vernis des instruments de musique: Principe et spécificités. In *Art et Chimie: Les Polymères*; CNRS Editions: Paris, France, 2002; pp. 75–80.
17. Lanterna, G.; Giatti, A. Caratterizzazione non invasiva delle vernici da ottone degli strumenti scientifici: Ricette storiche, realizzazione di provini verniciati, ricerca analitica e applicazioni "in situ" su strumenti storici. *OPD Restauro* **2014**, *26*, 165–180.
18. Salvadori, B.; Galeotti, M.; Porcinai, S.; Cagnini, A. Non-invasive FT-IR reflection to assess and monitor coatings on metals, In proceedings of the New strategies for diagnostics of conservation treatments conference, Amsterdam, The Netherlands, 7–8 February 2019.
19. Tripier-Deveaux, A.-M. *Traité Théorique et Pratique sur l'art de Faire les Vernis: Suivi de Deux Mémoires, l'un sur les Dangers Qui menacent les Peintures Vernies d'extérieurs, l'autre sur les Précautions à Prendre Pour Assurer aux Revernissages la Même Durée Qu'aux Vernissages Faits sur les Peintures Fraîches*; Librairie scientifique-industrielle de L. Mathias: Paris, France, 1845.
20. Société de l'École d'horlogerie de Paris; Chambre syndicale de l'horlogerie de Paris. *Revue Chronométrique*; Organe des Sociétés D'horlogerie et des Chambres Syndicales: Paris, France, 1876.
21. Roseleur, A. *Guide Pratique du Doreur, de L'argenteur et du Galvanoplaste: Manipulations Hydroplastiques*; Plazanet: Paris, France, 1873.
22. Rie (de la), E.R. Fluorescence of paint and varnish layers (Part I). *Stud. Conserv.* **1982**, *27*, 1–7. [CrossRef]
23. Mills, J.S.; White, R. *The Organic Chemistry of Museum Objects*; Butterworth & Co.: London, UK, 1987.
24. ISO 16474-3:2013. *Paints and Varnishes—Methods of Exposure to Laboratory Light Sources—Part 3: Fluorescent UV Lamps*; ISO: Geneva, Switzerland, 2013.
25. Simpson-Grant, M. The Use of Ultraviolet Induced Visible-Fluorescence in the Examination of Museum Objects, Part 2. *Conserve O Gram* **2000**, *1*, 1–4.
26. The Conservation and Art Materials Encyclopedia Online (CAMEO). Available online: <http://cameo.mfa.org/wiki/Rosin> (accessed on 10 February 2021).
27. Derrick, M.R.; Stulik, D.C.; Landry, J.M. *Infrared Spectroscopy in Conservation Science*; Getty Conservation Institute: Los Angeles, CA, USA, 1999.
28. Derry, J. Investigating Shellac: Documenting the Process, Defining the Product. A Study on the Processing Methods of Shellac, and the Analysis of Selected Physical and Chemical Characteristics. Master's Thesis, University of Oslo, Oslo, Norway, 2012.
29. Nakata, Y.; Murakami, S. *FTIR Talk Letter*; Shimadzu: Kyoto, Japan, 2010; Volume 15.